

PHOTOCHROMIC AND PHOTOREFRACTIVE
EFFECTS IN BISMUTH SILICON OXIDE
DOPED WITH IRON AND BISMUTH
SILICON OXIDE DOPED WITH
IRON AND GALLIUM

By

SUSAN PATRICIA HOEFLER

Bachelor of Science

Creighton University

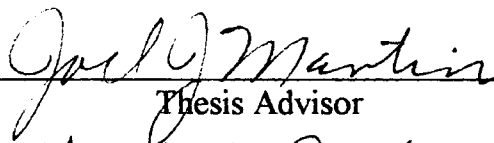
Omaha, Nebraska

1991

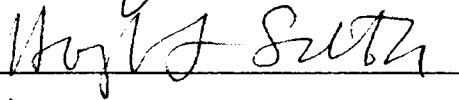
Submitted to the Faculty of the
Graduate College of the
Oklahoma State University
in partial fulfillment of
the requirements for
the Degree of
MASTER OF SCIENCE
July, 1994

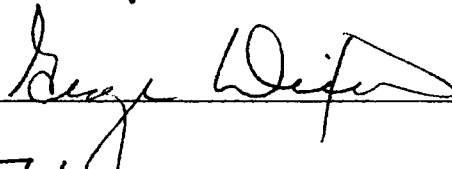
PHOTOCHROMIC AND PHOTOREFRACTIVE
EFFECTS IN BISMUTH SILICON OXIDE
DOPED WITH IRON AND BISMUTH
SILICON OXIDE DOPED WITH
IRON AND GALLIUM

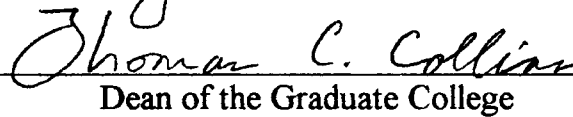
Thesis Approved:



Thesis Advisor







Dean of the Graduate College

ACKNOWLEDGMENTS

Throughout my graduate school experience, I have had the good fortune to come into contact with some very gifted teachers. Foremost, I wish to thank my “two” advisors, Dr. George Dixon and Dr. Joel Martin without whose support, both financially and mentally, this thesis would not have become a reality. Additionally, I wish to thank Dr. Dave Hart and Mr. Mike Hamilton who patiently served in the invaluable role of “dumb question buffer zone”.

Thanks goes to Mr. Charles Hunt for his infinite patience in teaching me how to grow good samples. I also wish to extend to Dr. Larry Scott a special thank-you for taking time from his busy schedule to serve on my graduate committee.

Finally, to my family, who have supported me throughout all my educational endeavors, I wish to simply say thank-you. No words can adequately describe my gratefulness for all of your support.

TABLE OF CONTENTS

Chapter	Page
I. INTRODUCTION.....	1
Defects.....	2
Photorefractive Effect.....	2
Statement of Purpose.....	5
II. EXPERIMENTAL PROCEDURE.....	6
Sample Growth.....	6
Absorption Measurements.....	7
Photorefractive Measurements.....	8
III. RESULTS AND DISCUSSION.....	10
Photochromic Curves.....	10
Photorefractive Data.....	20
IV. CONCLUSION.....	32
REFERENCES.....	33
APPENDICES	
APPENDIX A- DVM Data Acquisition Program Listing.....	35

LIST OF FIGURES

Figure	Page
1. Energy level diagram showing the proposed transitions responsible for the photochromic bands and the photorefractive data.....	4
2. The experimental setup for measurement of photorefractive effects in BSO:2%Fe and BSO:2%Fe5%Ga.....	9
3. Comparison of the baseline photochromic bands of undoped, Al-doped, Fe-doped, and FeGa-doped BSO.....	11
4. Photochromic absorption bands for BSO:2%Fe.....	14
5. Photochromic absorption bands for BSO:2%Fe5%Ga.....	15
6. The change in the absorption spectra for BSO:2%Fe.....	16
7. The change in the absorption spectra for BSO:2%Fe5%Ga.....	17
8. The isochronal anneal contour plot for BSO:2%Fe.....	18
9. The isochronal anneal contour plot for BSO:2%Fe5%Ga.....	19
10. The photorefractive temperature dependence of BSO:2%Fe.....	22
11. The 500 ms photorefractive temperature dependence of BSO:2%Fe5%Ga	23
12. The 2000ms photorefractive temperature dependence ofBSO:2%Fe5%Ga	24
13. 2000 ms photorefractive temperature dependence rescaled to 500 ms.....	25
14. DVM real-time plot of refracted signal from BSO:2%Fe and BSO:2%Fe5%Ga.....	26
15. Shutter runs at room temperature for BSO:2%Fe.....	27

Figure	Page
16. Shutter runs at room temperature for BSO:2%Fe5%Ga.....	28
17. 1000 ms shutter runs for BSO:2%Fe.....	30
18. 1000 ms shutter runs for BSO:2%Fe5%Ga.....	31

CHAPTER 1

INTRODUCTION

Bismuth silicon oxide, $\text{Bi}_{12}\text{SiO}_{20}$, and Bismuth germanium oxide, $\text{Bi}_{12}\text{GeO}_{20}$, hereafter referred to as BSO and BGO, are members of the sillenite family of crystalline compounds. These unique crystals have considerable potential for a wide variety of technological applications, namely, optical data processing¹⁻³, real time interferometry⁴, nonlinear optical applications^{2,5}, and as storage media in holographic memory systems^{6,10}. These materials exhibit a large photorefractive effect, a change in the refractive index induced by light⁶⁻⁹, which supports a large number of emerging applications. For this reason, BSO and BGO, are being studied extensively. A necessary preliminary step in the understanding of these materials is to characterize the defect structures of these materials.

BSO and BGO are closely related materials. Both have the same body-centered cubic structure, first studied by a Swedish chemist named Sillen⁹, and have a symmetry that correspond to the $m\bar{3}$ point groups, which lack inversion symmetry^{9,11}. Room temperature studies of BGO were undertaken by Abrahams et al.¹². The unit cell consists of a Ge/Si atom surrounded by four oxygens in a tetrahedral geometry. This combination occurs at all eight corners of the cube and at the center of the cube. Bismuth atoms within the cube have seven oxygen atoms arranged in a distorted octahedral geometry around each⁹. Due to the lack of inversion symmetry, BSO is piezoelectric and electro-optic. These electro-

optic properties, in addition to the defects inherent in the crystal, combine to produce the photorefractive effect.

Defects

A serious problem in the production of these crystals is that the internal defect structure, a combination of electrons or holes trapped at impurities and other defects¹³, differs depending on the source of the crystals. Quality crystals have been produced by growth in air using the Czochralski method, producing crystals with a yellow coloration¹⁴, and hydrothermal techniques; resulting crystals are colorless and have a much lower trap density than Cz materials¹⁵. BSO crystals are normally grown using the Czochralski method. The resulting yellow color is attributed to the presence of a deep electron donor, possibly a bismuth occupying a silicon site¹⁴. This anti-site bismuth would act as a donor. Hou et al¹⁶ postulate that the donor is due to an electron occupying a silicon vacancy complex. Oberschmidt¹⁷ originally argued on the basis of enthalpy measurements for the improper occupation rather than a vacancy. More recent work by Craig and Stephenson¹⁸ support this possibility. They found that the compound $\text{Bi}_{25}\text{FeO}_{40}$ has the same structure as BSO with Fe on one Si site and Bi on the other in the unit cell.

Photorefractive Effect

The electrons (or holes) trapped at the impurities can be excited into the conduction (or

valence) band by exposing the crystal to light. Once in the conduction band, the electrons migrate until they recombine at an empty shallower trap. Figure 1 shows an energy level diagram depicting the proposed charge migrations that occur when BSO is illuminated with near band edge light. Exposure at low temperatures to band edge light produces photochromic absorption bands. BSO doped with iron or BSO doped with iron and gallium each contains unique acceptor states that create the absorption shoulders found in their photochromic curves. Figure 1, (b) and (c), also shows proposed energy levels for these acceptor states. If the exposure to light is nonuniform, such as in a four-wave mixing experiment using crossed laser beams, a nonuniform charge redistribution results. This distribution of charge produces a complementary electric field pattern within the crystal. In noncentrosymmetric crystals, like BSO, the field produces a corresponding pattern in the index of refraction through the electro-optic effect^{6,8,14}. This pattern in the index of refraction, or grating, is known as the photorefractive effect. The lifetime of the grating depends largely upon the material, but also on the temperature, and the wavelength and intensity of the “write” or exposure beam.

In addition to undoped BSO, recent studies have included BSO doped with 2% Fe and also BSO doped with 2% Fe and 5% Ga. The purpose of the dopants is to provide information on the compensation of the deep donor through the resulting changes in the absorption spectra and the changes in the charge distribution in the photorefractive effect.

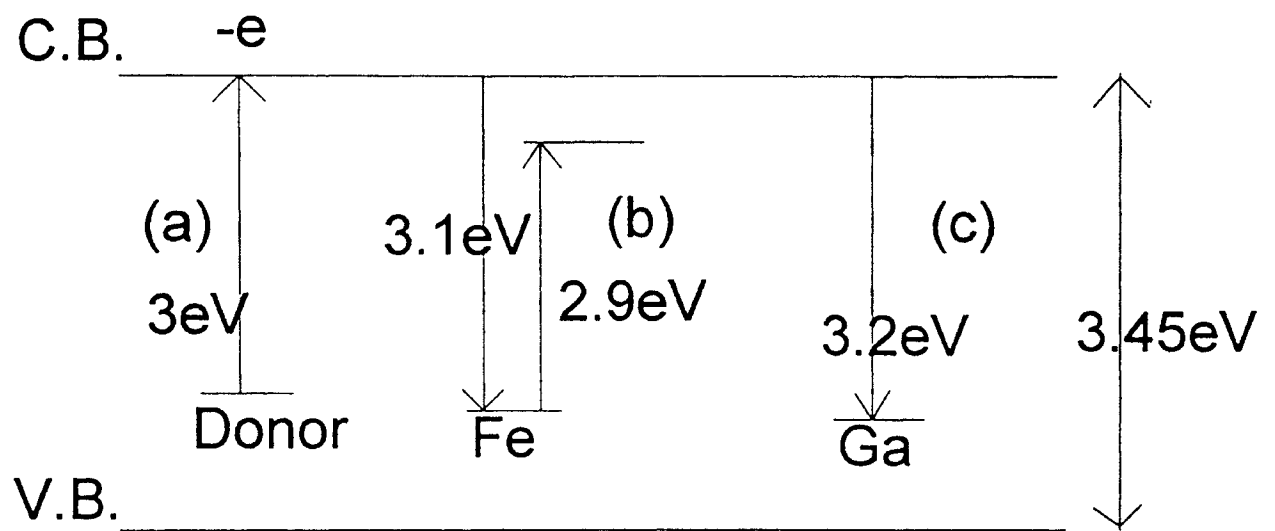


Figure 1. Energy level diagram showing the proposed transitions responsible for the photochromic bands and the photorefractive data.

Statement of Purpose

BSO:2% Fe and BSO:2% Fe 5%Ga form photochromic absorption bands when exposed to 3eV, near band edge, light. In four-wave mixing experiments, both crystals exhibit the ability to form gratings. In the following experiment, a systematic study of the low temperature absorption bands, the isochronal anneals, and the physical properties of the photorefractive gratings for both BSO: Fe and BSO: FeGa are presented. Comparison of the absorption bands and the photorefractive data help to characterize the defect structures of these crystals. Ultimately this information will bring a better understanding of BSO and allow for utilization in technological applications.

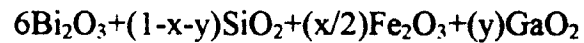
CHAPTER 2

EXPERIMENTAL PROCEDURE

For this study two doped samples were grown at Oklahoma State University using the Czochralski method. The first was a 2% iron-doped BSO sample. Iron doping was accomplished by adding iron-oxide to the melt with a corresponding reduction in SiO₂ by the following ratio:



The second sample to be grown was doped with 2% Fe and 5% Ga by the following formula:



The chemicals used were Johnson-Matthey Grade-1 bismuth oxide (Bi₂O₃) and silicon oxide (SiO₂).

Sample Growth

Both chemical mixtures were prepared for the melt by undergoing first, a mixing period in a glass container for 48 hours, then the mixture was transferred to a platinum crucible and heat treated at 800° C surrounded by a flowing oxygen atmosphere for another 48 hours. Upon removal, the platinum crucible containing the mixture was placed in a 20 kW 450 kHz RF induction furnace where it was heated to approximately 900° C. Once the mixture was melted, an orientated seed crystal of undoped BSO was dipped into the melt and slowly withdrawn. The seed was rotated at 30 to 86 revolutions per minute to prevent the formation of a darker center or core¹⁹. The

temperature of the melt was monitored by an Acufiber model 10 controller that uses a sapphire sensor in contact with the base of the crucible. The temperature set points, the temp-time controlled growth period, and the warm-up/cool-down ramp were controlled by an HP-86 microcomputer. The seeds for each of the two samples were [100] oriented Oklahoma State University Czochralski grown BSO. At the end of the growth period, the newly grown crystals were cooled to room temperature over a period of 48 hours to prevent cracking due to thermal stress.

Optical samples 1-1.5 mm thick were cut from the crystals. Both (100) and (110) surfaces were cut. Surfaces 90° degrees to the c-axis were used for absorption measurements, samples cut 45° degrees to the c-axis were utilized for photorefractive measurements.

Absorption Measurements

For the absorption measurements, the samples were mounted on the cold finger of a CTI closed-cycle cryogenic refrigerator at a 45° angle to the sample beam of a model 330 Perkin Elmer spectrophotometer. The 45° angle allowed the polished samples to be exposed to the excitation light beam without having to remove the cold-head from the spectrophotometer. All optical absorption scans were made at 9-15 K. Before scanning, the samples were exposed to near band edge light, at 8-15 K, using an Oriel 200-W Xe lamp and a Spex Minimate monochromator with 5 mm slots. The near band edge light “writes” photochromic bands in the samples. The scans using the spectrophotometer are used to optically characterize the samples in their as-grown conditions.

Then, the thermal stability of these photochromic bands are tested by performing a series of isochronal anneals. After collecting an absorption spectrum at 8-15 K the temperature of the sample, using the refrigerator, is raised to the desired value and then returned to 8-15 K for the next absorption scan.

Photorefractive Measurements

The samples cut 45° degrees to the c-axis were used in an experiment designed to measure photorefractive effects. A 442 nm Helium Cadmium laser beam was split in a beam splitter. The resulting two beams were bent back towards the cold finger mounted sample. When the beams reached the sample they were crossed to form a grating inside the sample. The sample was oriented perpendicular to the incoming beams. The resulting grating was “read” by a 632.8 nm Helium Neon laser. This “read” beam was geometrically oriented at the Bragg angle, approximately 9°, and the resulting refracted beam was fed into a photomultiplier tube, channeled into a Hewlett Packard digital scope and a Keithley Digital Multimeter, and finally analyzed by an IBM 286 personal computer. The Helium Cadmium beam, or “write” beam, is sent through a shutter before it hits the beam splitter. This allows the “write” time to be predetermined. Other predetermined variables are: the intensity of the “write” beam, the intensity of the “read” beam, through use of various neutral density filters, and the temperature of the sample by using a CTI Cryogenic refrigerator. A schematic diagram of the experimental setup is found in Figure 2.

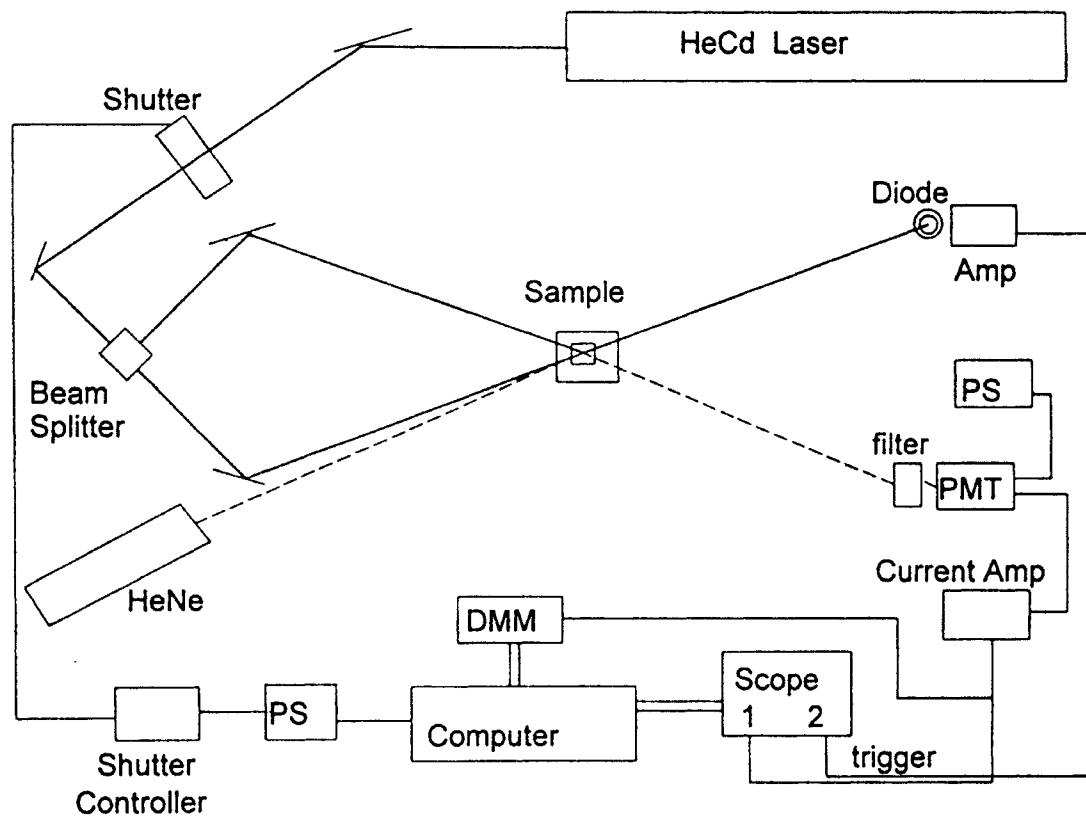


Figure 2. The experimental setup for measurement of photorefractive effects in BSO:2%Fe and BSO:2%Fe5%Ga.

CHAPTER 3

RESULTS AND DISCUSSION

Photochromic Curves

Figure 3 shows absorption spectra taken at 10 K on undoped, Al-doped, Fe-doped, and FeGa-doped samples. These curves serve as the baselines or background for the photochromic data. The important differences between these samples occur at the absorption shoulders around 3.3 eV for Al and near 3 eV for the other three curves. The Al-doped sample is a nearly colorless crystal. The dopant occupies the Si site and acts as an acceptor to compensate the deep donor (see figure 1, (a)) and thus removes the yellow coloration²⁰. The curve for the undoped sample shows the absorption shoulder near 2.9-3 eV which causes the yellow color typical of BSO and BGO. The shoulder is thought to be due to excitations from the deep donor, in Fig. 1, to the conduction band. This shoulder is missing (or at least greatly reduced) in the Fe, Al and FeGa-doped specimens. The absorption cut-off in the Al-doped sample is at 3.3 eV. Hart *et al.*²⁰ found the Ga-doped BGO also cut-off at 3.3 eV. These results suggest that the Al and Ga acceptor levels are about 3.3 eV below the band edge. Doping with Fe and with FeGa, also removes the yellow color, but the absorption cut off is between 3 eV and 3.2 eV. Since the FeGa-doped sample had enough Ga to fully compensate the donor, its cut-off would be expected to be near 3.3 eV²⁰. Thus, it appears that the cut-off is due to an internal transition in the Fe, perhaps from the spin 5/2 ground state to the spin 3/2 excited state.

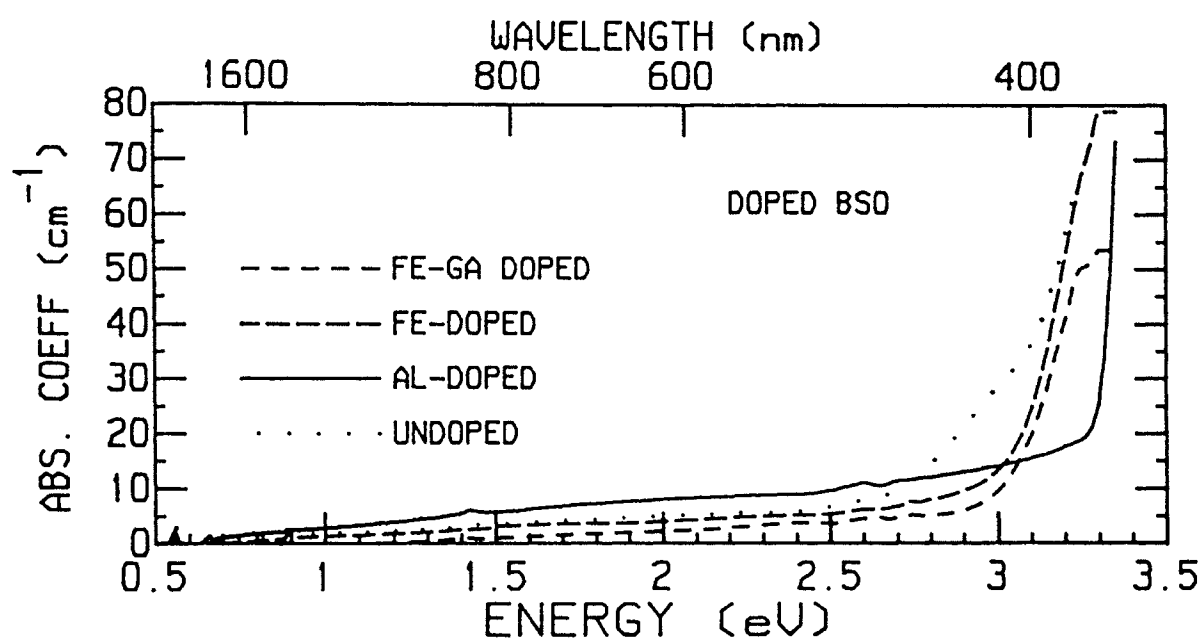


Figure 3. Comparison of the baseline photochromic bands of undoped, Al-doped, Fe-doped, and FeGa-doped BSO.

This excited state would be located within the band gap, but would be very close to the conduction band²¹. This could possibly allow for thermal excitation at room temperature of these electrons into the conduction band. Thermal excitation may account for a winking phenomenon noticed in both the Fe-doped BSO and FeGa-doped BSO samples. This will be discussed in more detail later.

Figures 4 and 5 show absorption curves in Fe-doped and FeGa-doped BSO after irradiation using 3eV light from the Oriel 200W Xe lamp. The irradiation was applied in increments up to a total of 60 minutes for the Fe-doped sample, and up to a total of 90 minutes for the FeGa-doped sample. There was a noticeable growth in signal strength in the shoulder region in both samples.

In figures 6 and 7, the baseline was subtracted from the absorption curves in figures 4 and 5 and the resulting change in absorption for each illumination time was graphed. The growth in absorption for the Fe-doped sample is not centered at a specific energy. Instead, there is a spread of energies from 2.5 eV-3.2 eV that are affected. There is also a small peak at 1.4 eV. This corresponds to the results of Hart *et al.*²⁰. BGO:4%Ga has a peak at 1.55 eV and BGO:5%Al has a peak at 1.38 eV. These two also have a broad, relatively featureless band centered around 2.45eV. The Fe-doped band appears to be centered closer to 2.8 eV.

In addition to these peaks, BGO: Al and BGO: Ga each have a characteristic peak at 1 eV, and 1.1 eV, respectively. These peaks are thought to be due to the addition of the dopants into the material. By analogy with quartz, the proposed mechanism is the hole center. The corresponding hole center peak in the FeGa-doped sample is absent. The

FeGa-doped sample however, has peaks at 2.2 eV and 3.3 eV but no peak at 1.4 eV.

There is growth in the 2.5eV-3.2eV range that corresponds with the Fe-doped sample.

In figures 8 and 9 the isochronal anneal graphs are shown. These contour plots show the decay of the photochromic bands. In Fe-doped, the bands decay between 125K and 150K. In 4%Ga-doped BGO, the infrared bands (1.1 and 1.55 eV), and a major portion of the visible range anneals between 100 and 120 K. Al-doped BGO is similar except the anneal occurs in the 80-100 K range. The remaining visible range absorption decays just below 230 K²⁰. In FeGa-doped, there seems to be only a small decay at 300K. No higher temperature studies were performed; however, future work should include higher temperature anneal studies on the FeGa-doped samples.

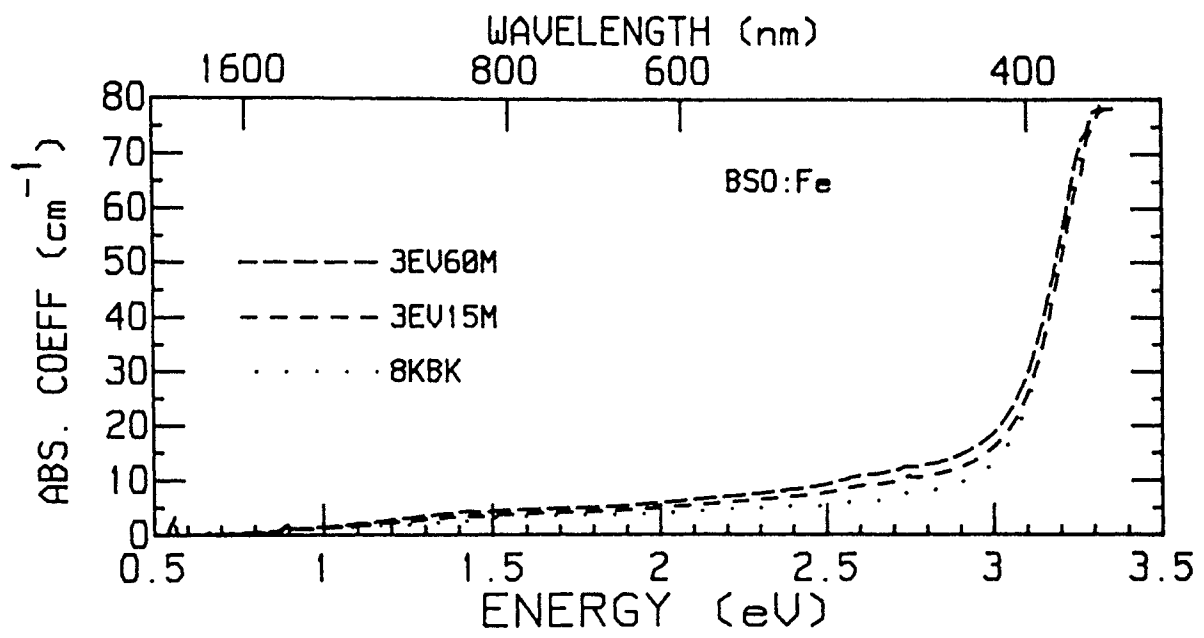


Figure 4. Photochromic absorption bands for BSO:2%Fe

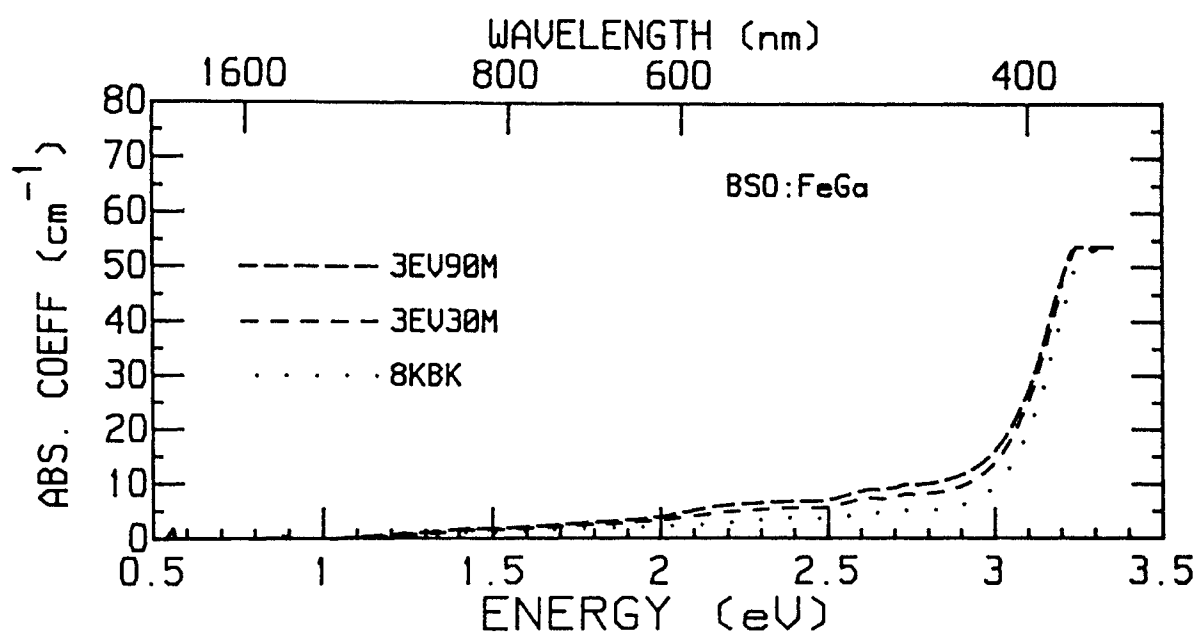


Figure 5. Photochromic absorption bands for BSO:2%Fe5%Ga

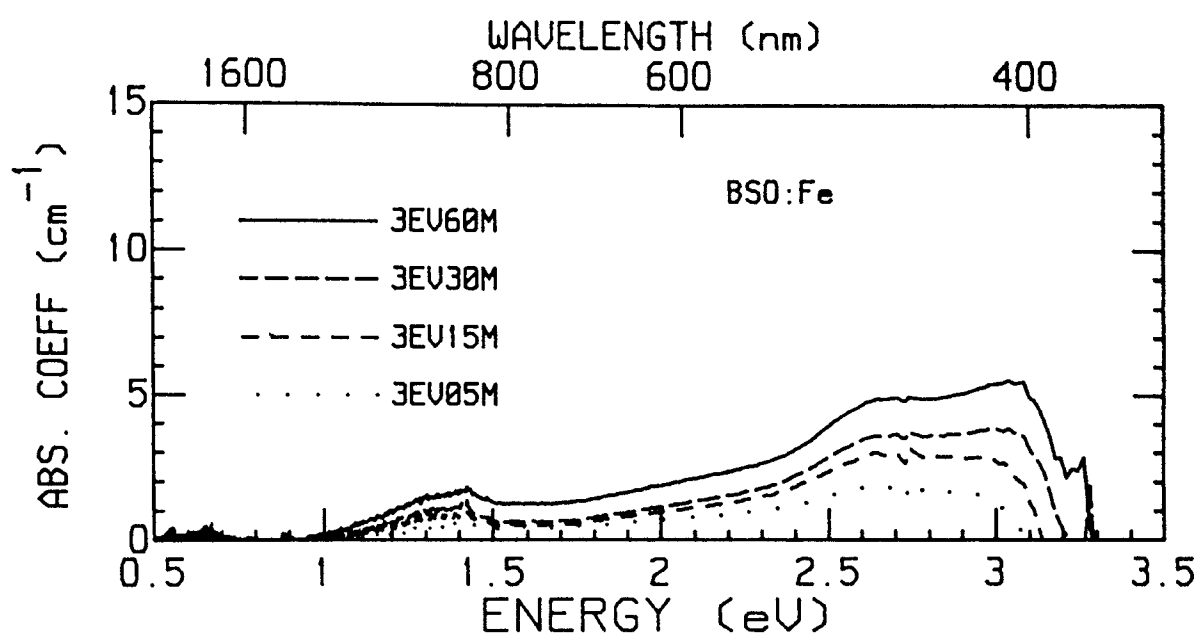


Figure 6. The change in the absorption spectra for BSO:2%Fe

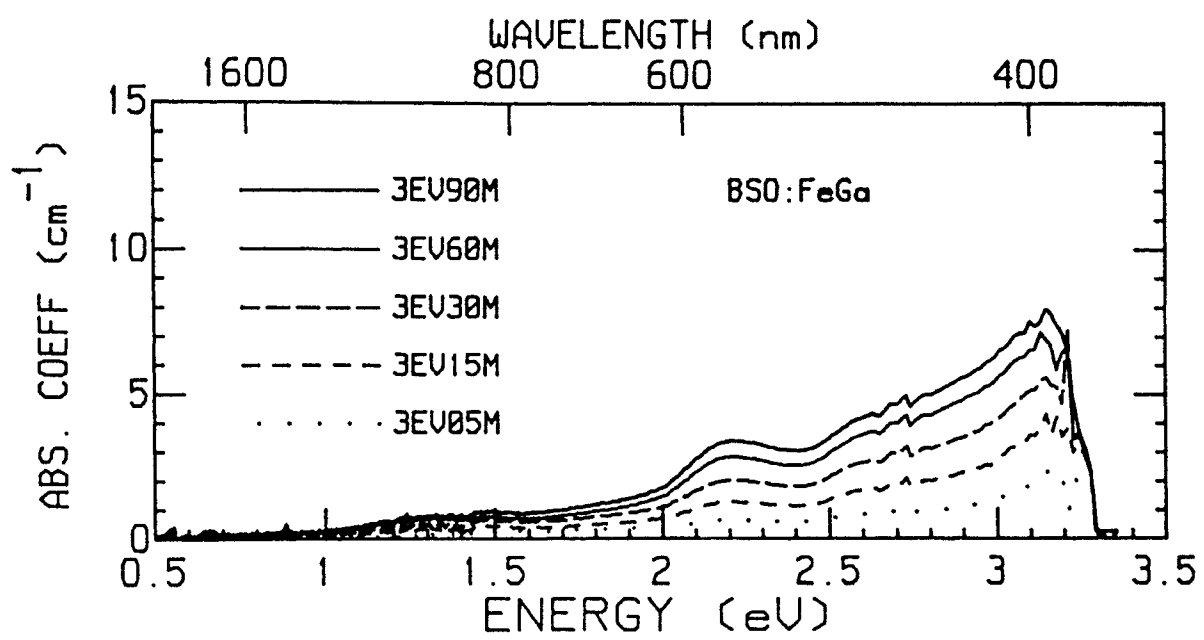


Figure 7. The change in the absorption spectra for BSO:2%Fe5%Ga

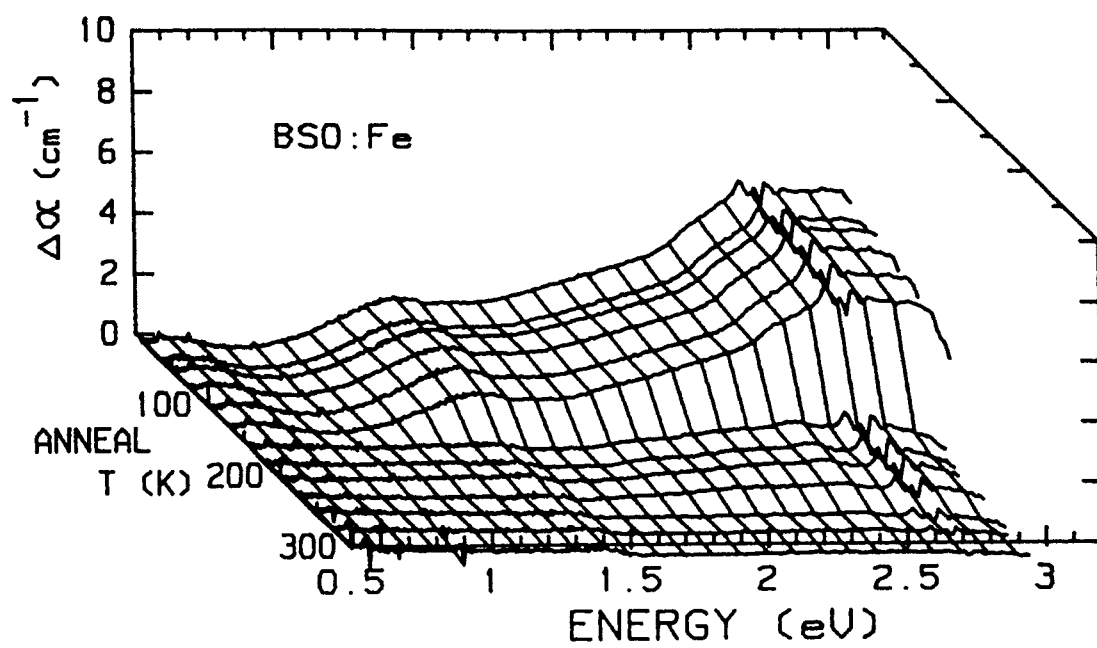


Figure 8. The isochronal anneal contour plot for BSO:2%Fe

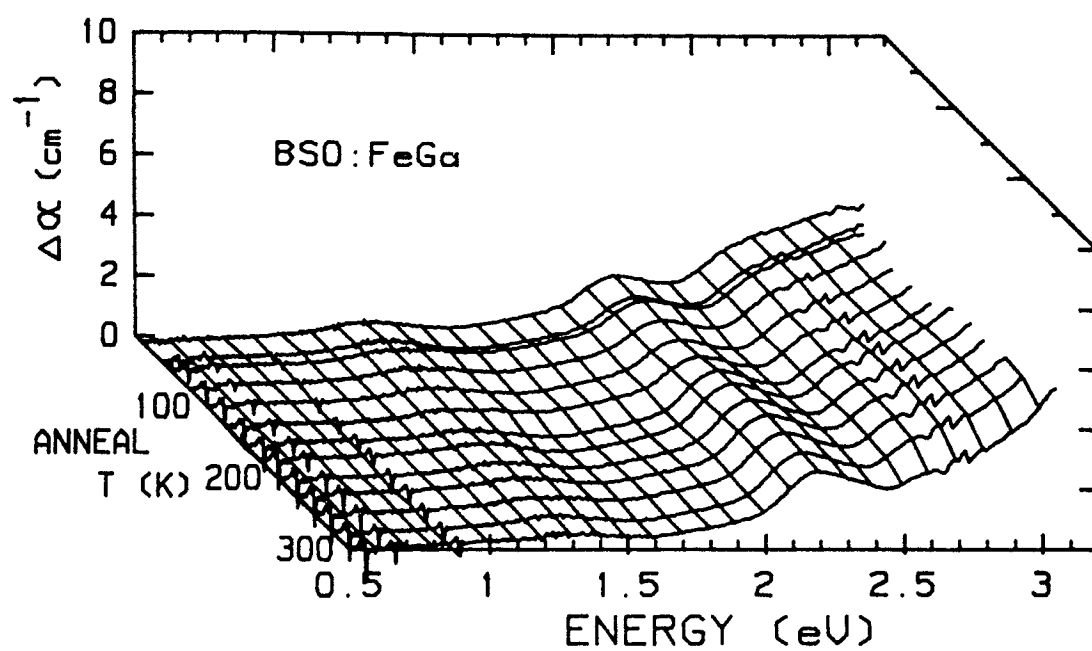


Figure 9. The isochronal anneal contour plot for BSO:2%Fe5%Ga

Photorefractive Data

Figure 10 shows the temperature dependence of the grating during the “write” process of BSO:Fe. The shutter time was 100ms. The grating spacing was measured at 2μ . At 300K there is an initial peak which decays through 200K. This leading peak may occur due to the increase in mobility at room temperature or thermal excitations. At 150K, however, there is a sudden rise in the observed signal. This rise correlates with the decay of the photochromic bands between 125K and 150K in Fig. 8. There is also a correspondence with the disappearance of the ESR Fe^{3+} signal¹³. Foldvari *et al.*²² have found that the BGO:Fe photorefractive signal at room temperature has a different origin from the signal seen at low temperatures.

Figures 11, 12, and 13 show the temperature dependence of BSO:FeGa at different write times. Figure 11 was done with a shutter time of 500ms. Figures 12 and 13 are for the same shutter time of 2000ms. Figure 13 shows the first 500 ms of the 2000 ms data as a comparison for figure 11. The data between the two separate trials appear to be in good agreement. Note that the overall signal strength of the FeGa-doped sample is less than the Fe-doped signal in the first 100ms of the temperature dependence. The FeGa-doped response time, in terms of signal rise, was slower than that of the Fe-doped. Since both Fe and Ga are acceptors with nearly the same energy in the band gap, it is possible that they are “competing” for electrons. Also, the energy of our laser, 442nm, is not enough to create photochromic bands in Ga-doped BSO²⁰. It is possible that mainly the Fe is being affected during the temperature dependence “write” trials.

From Fig. 12, the sudden rise in signal can again be seen at low temperature.

However, this time it appears at 100K. There is no direct correlation between this rise and the isochronal anneal decay of Fig. 9. There is also an initial peak at 300K which smooths out by 225K. More study is needed to sort out the dynamics of the charge transfers taking place.

In addition to the temperature dependence studies, the winking phenomena mentioned earlier was investigated. The DVM was programmed to receive data for extended periods of time. This data was plotted on a personal computer real-time. The program used is reproduced in Appendix A. The plotted results are shown in Fig. 14. The winking may be attributed to the presence of iron in both of the samples²³. The BSO:Fe sample showed the phenomena to a lesser degree than the BSO:FeGa sample. If indeed an internal ground to first excited state transition is occurring, the electrons in the excited state may be thermally excited into the conduction band at room temperature.

In Figs. 15 and 16, the change in the signal at room temperature for increasing shutter times is shown for both Fe-doped and FeGa-doped samples respectively. Both of the samples show the same trend to smoothly peak and then decrease in signal intensity. Fe-doped peaks at room temperature between 300-500 ms. FeGa-doped, however, shows max intensity at 500ms.

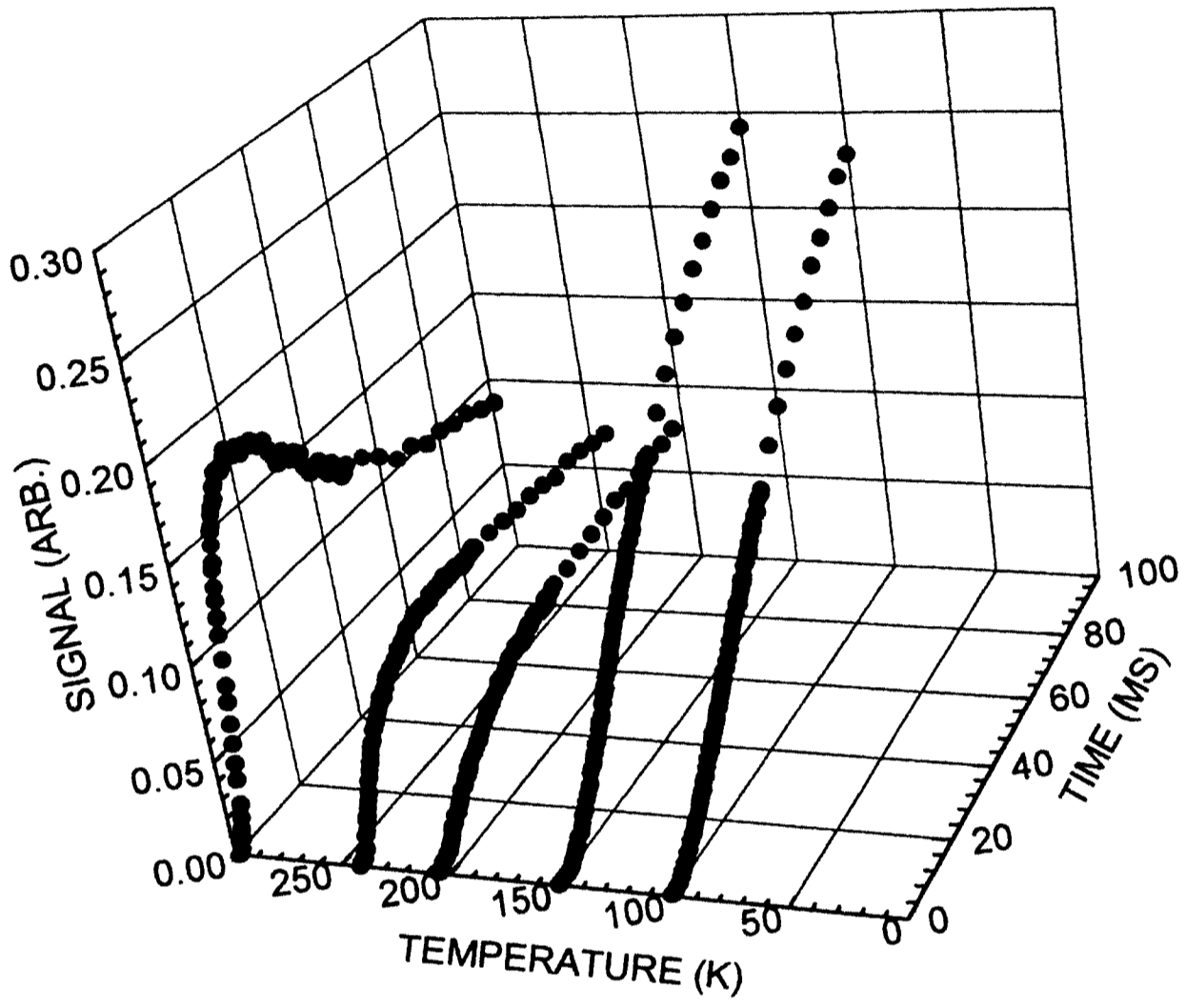


Figure 10. The photorefractive temperature dependence of BSO:2%Fe

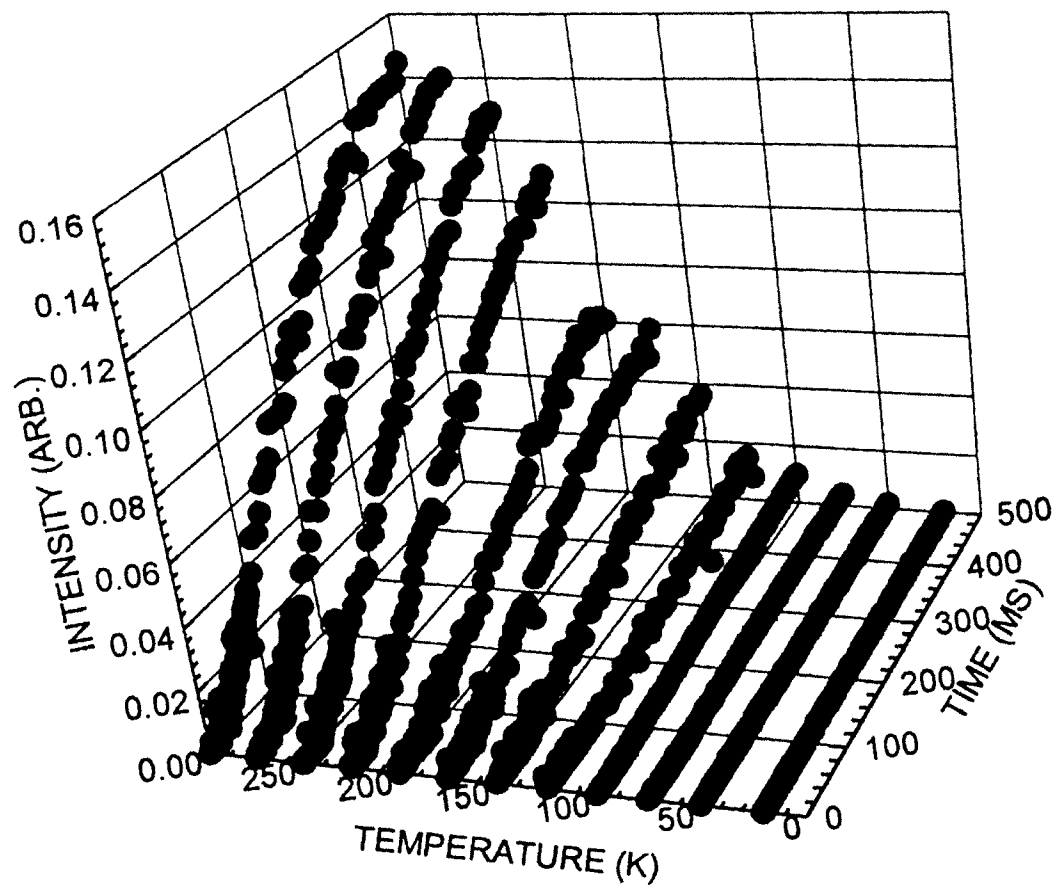


Figure 11. The 500ms photorefractive temperature dependence of BSO:2%Fe5%Ga

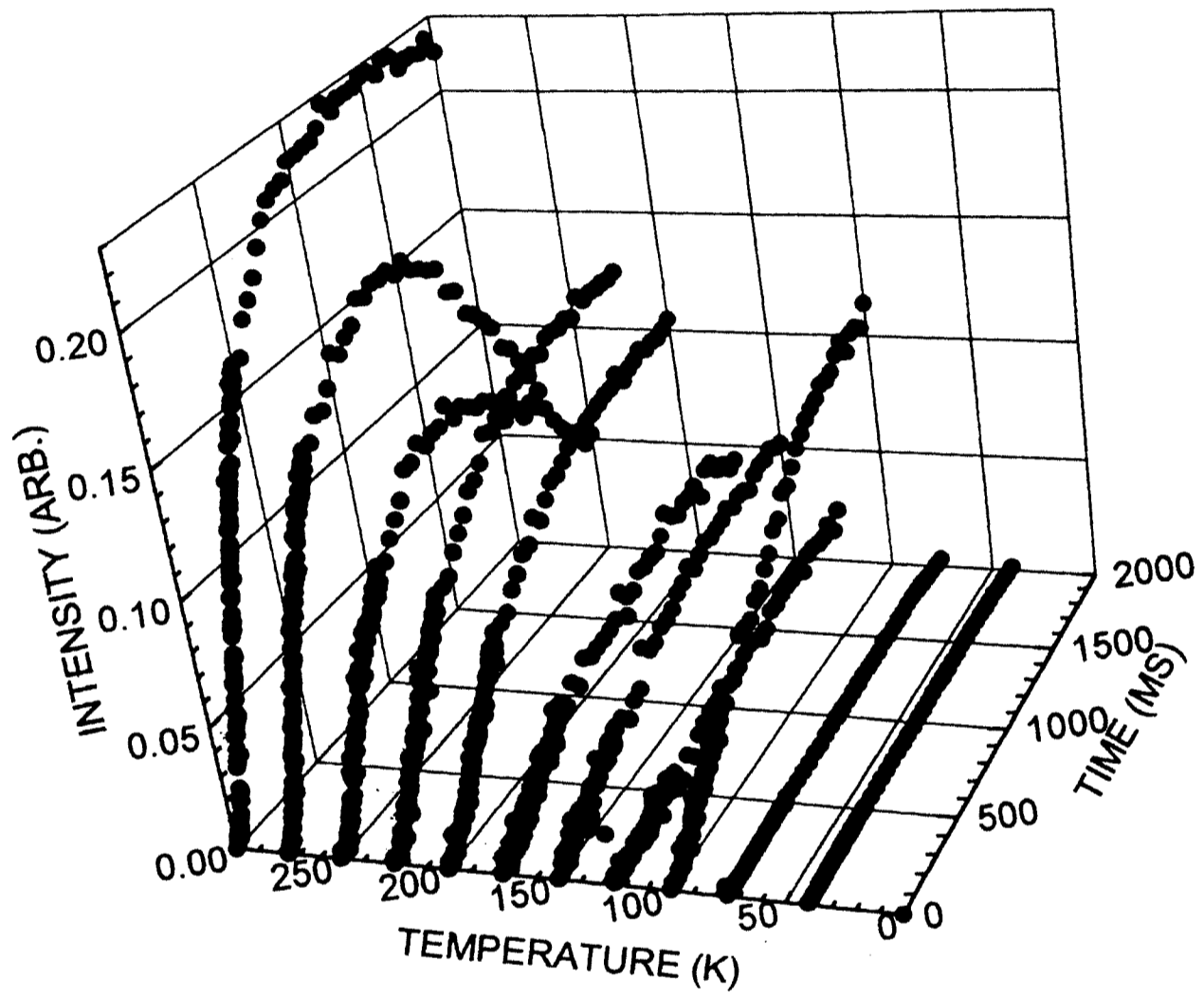


Figure 12. The 2000ms photorefractive temperature dependence of BSO:2%Fe5%Ga.

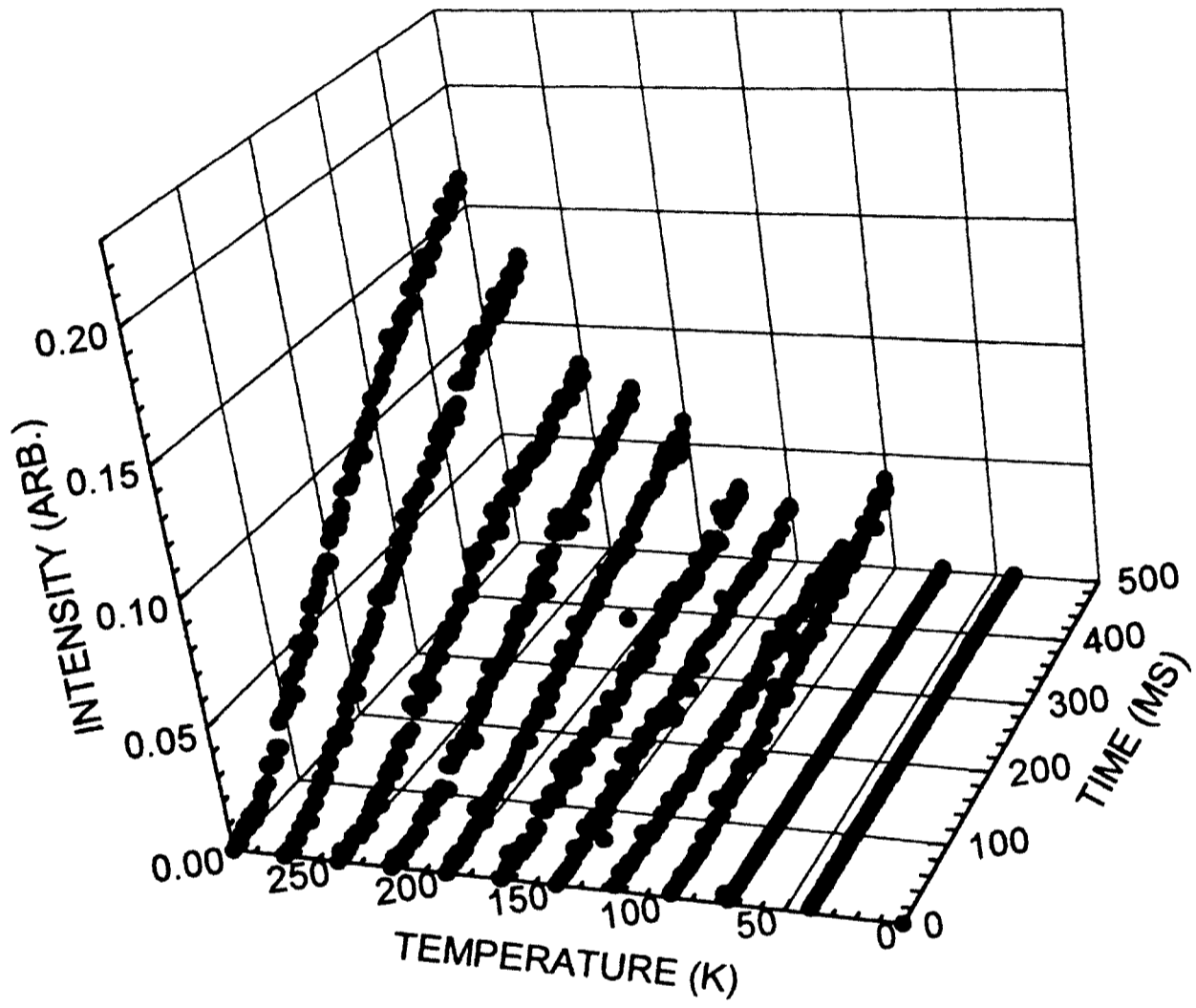


Figure 13. 2000ms temperature dependence rescaled to 500ms

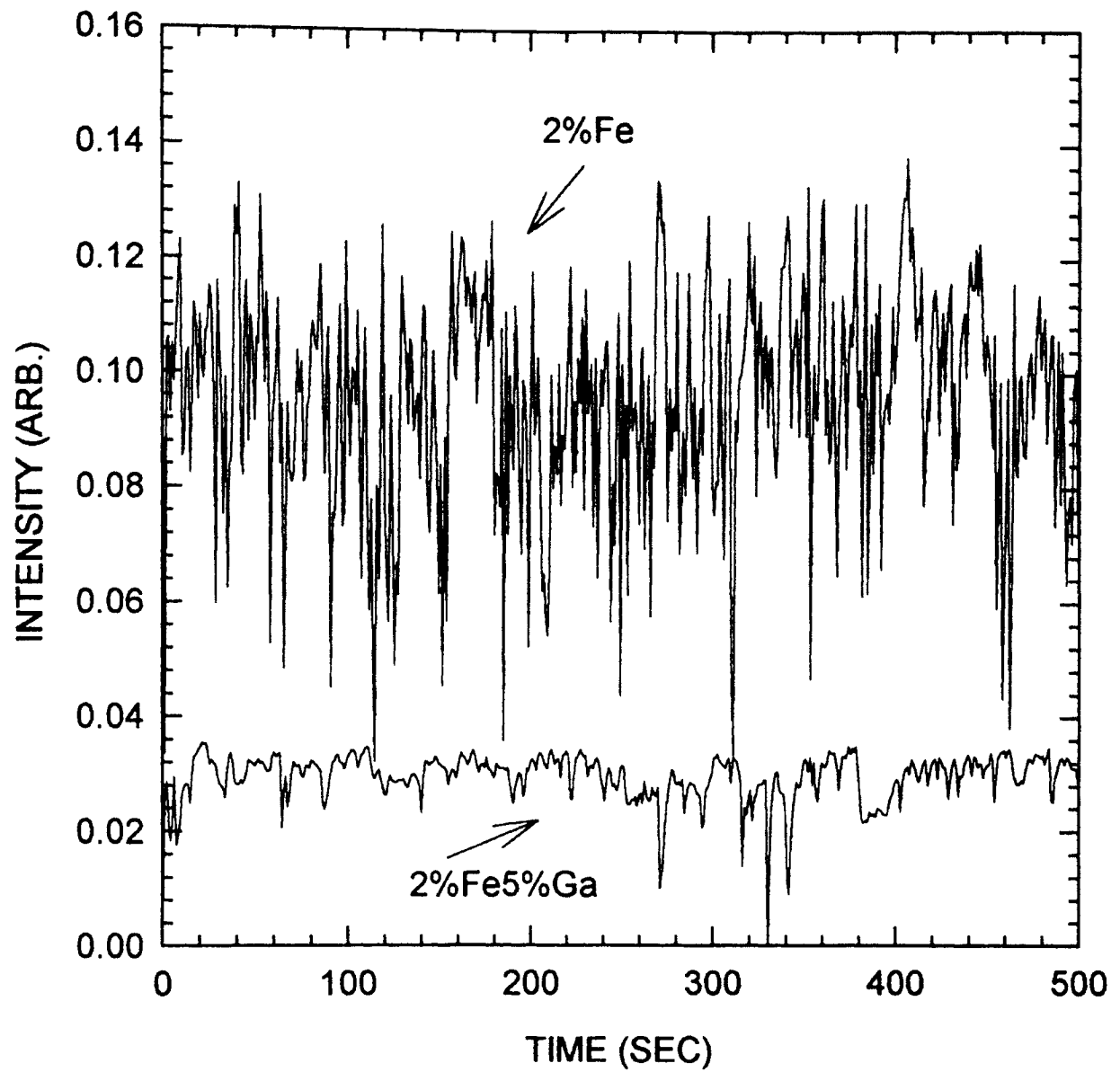


Figure 14. DVM real-time plot of refracted signal from BSO:2%Fe and BSO:2%Fe5%Ga

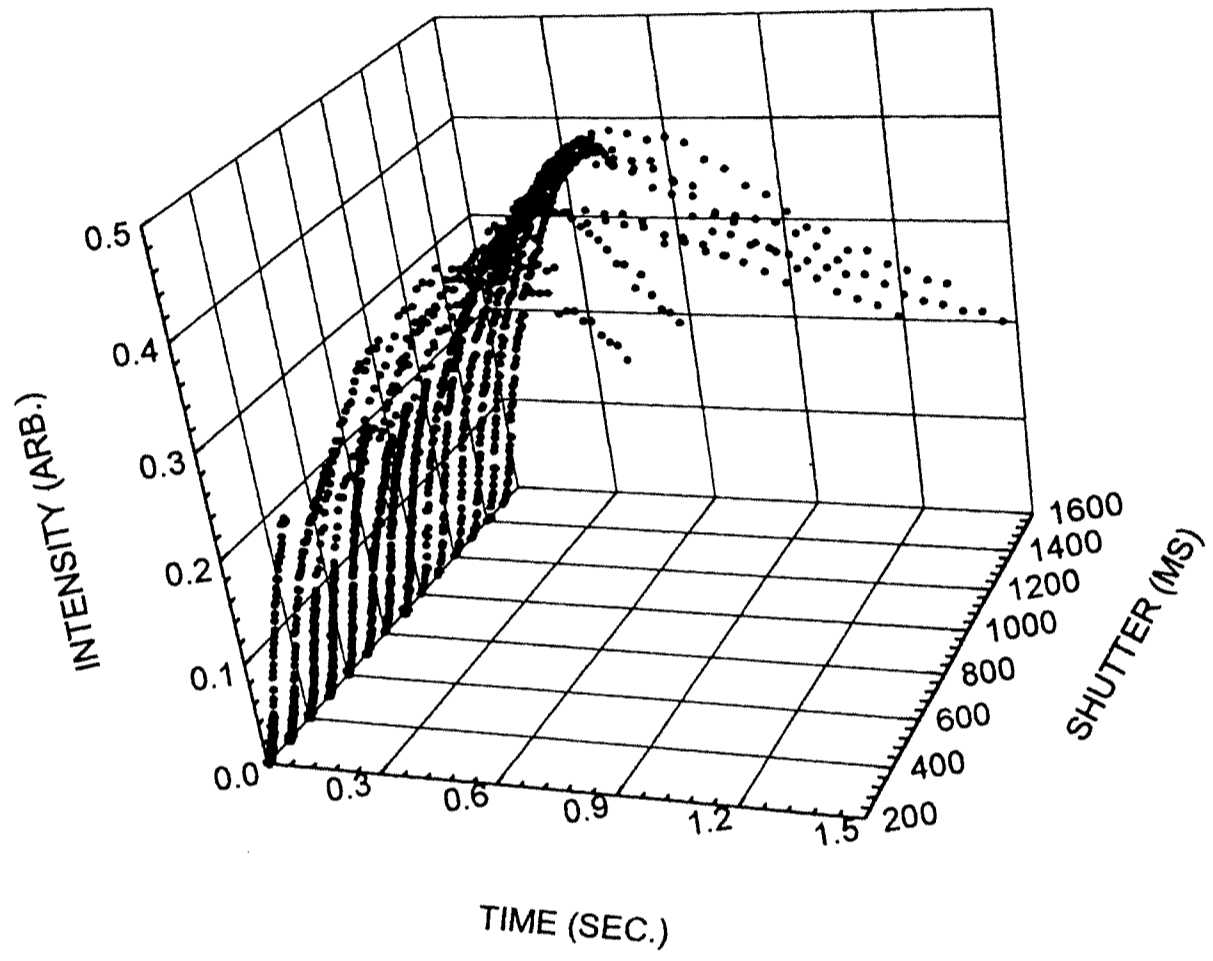


Figure 15. Shutter runs at room temperature for BSO:2%Fe

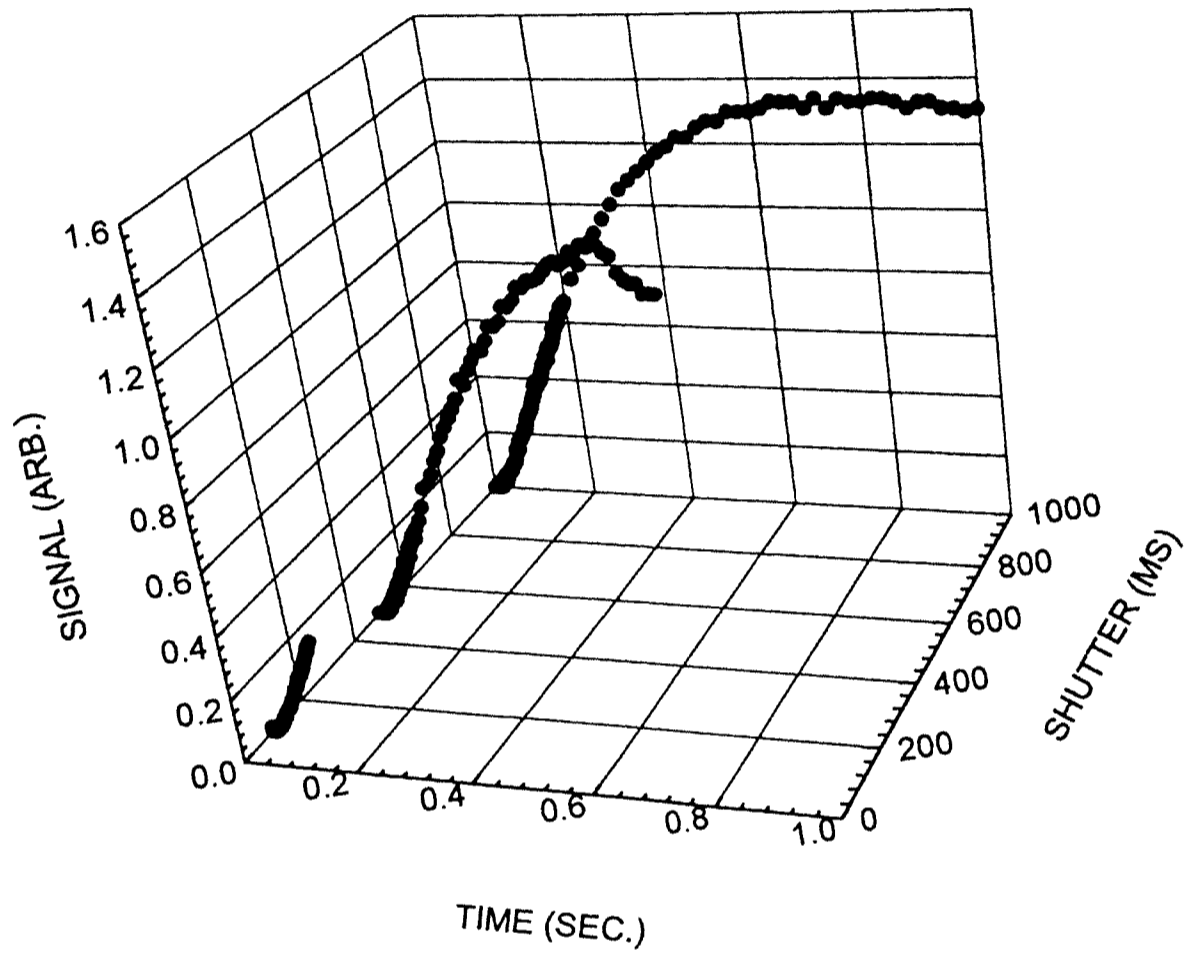


Figure 16. Shutter runs at room temperature for BSO:2%Fe5%Ga

Finally, to monitor the reproducibility of the data, the shutter was opened for 1000ms and consecutive readings were taken. This was done on both the BSO:Fe and the BSO:FeGa samples. The readings were taken immediately after each other at room temperature. Results are shown for Fe-doped in Fig. 17 and for FeGa-doped in Fig. 18. For the majority of trials, the results were close, however, in figure 18, there was one trial with a signal intensity that went off scale. It seems that signal intensity is largely dependent on the prior “immediate” history of the sample and possibly longer term effects not measured in this study

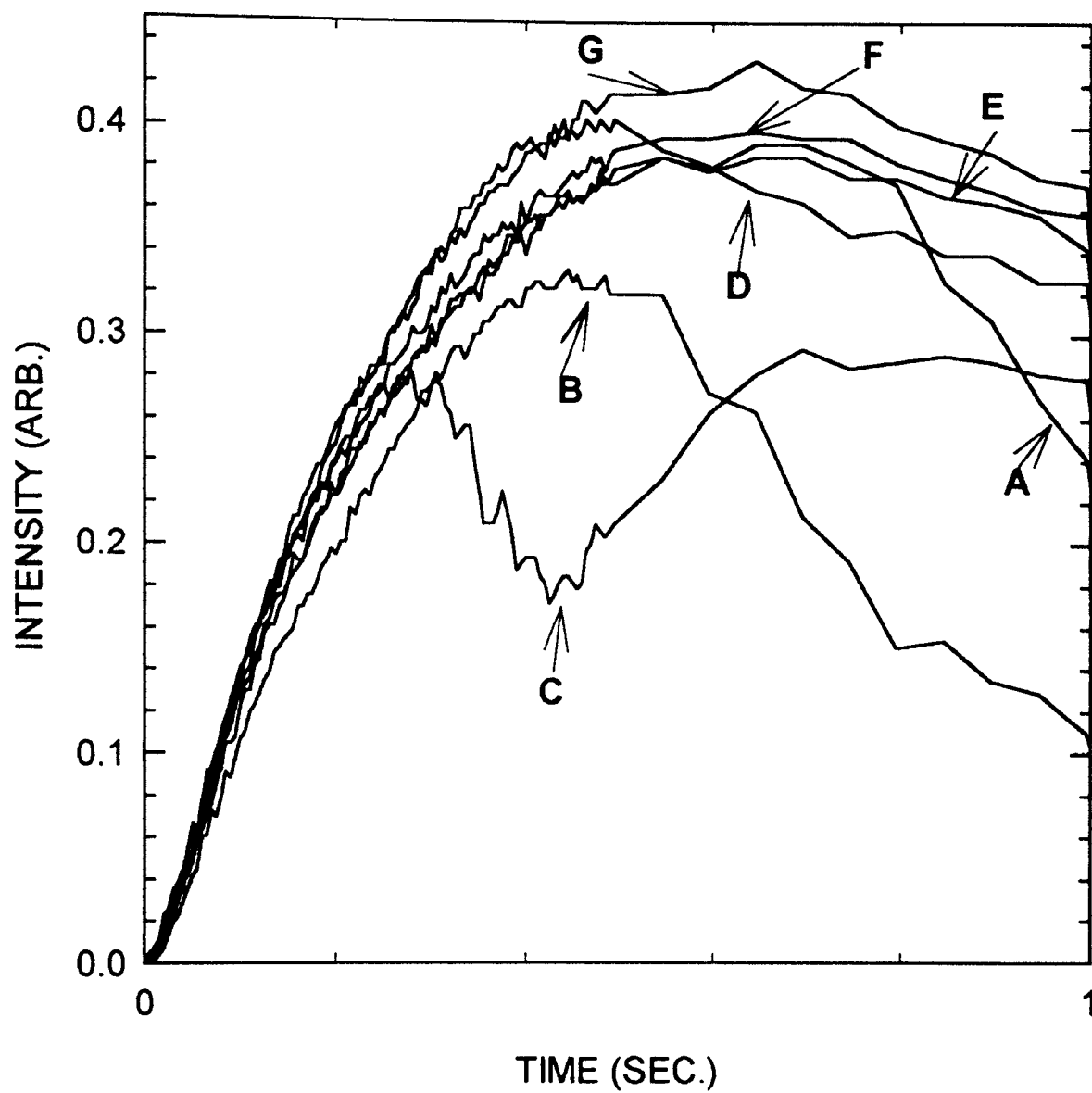


Figure 17. 1000ms Shutter runs for BSO:2%Fe

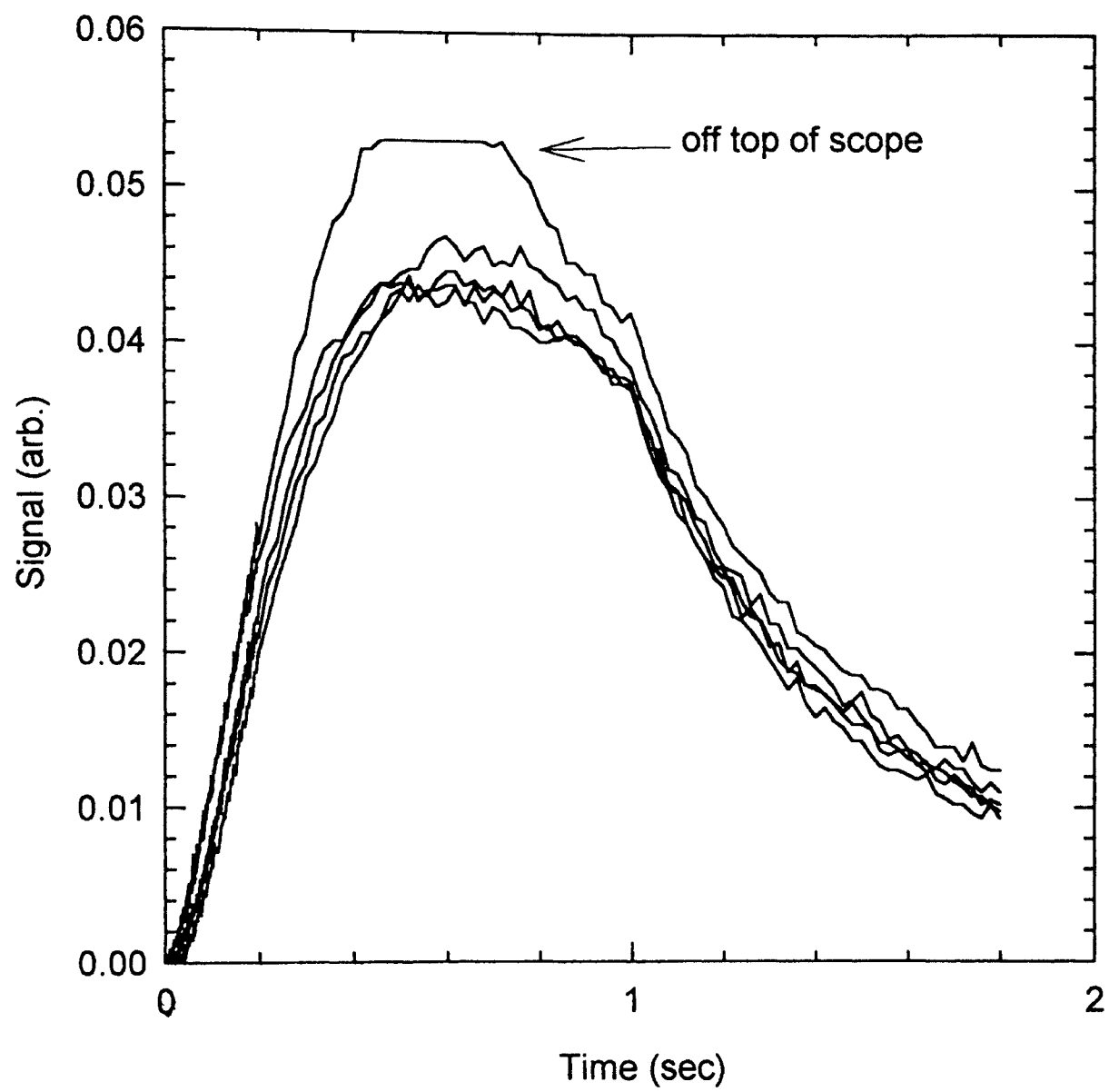


Figure 18. 1000ms Shutter runs for BSO:2%Fe5%Ga

CHAPTER 4

CONCLUSION

BSO:2%Fe and BSO:2%Fe5%Ga form photochromic absorption bands at low temperatures. These photochromic curves show interesting results at the absorption shoulders when compared with undoped BSO and Al-doped BSO. Undoped BSO, yellow in color, exhibits a strong absorption shoulder due to the presence of charge migrations from a deep donor to the conduction band. Al-doped BSO, however, has an absorption cut-off at 3.3 eV and is a nearly colorless crystal. The dopant occupies the Si site and acts as an acceptor to compensate the deep donor and thus removes the yellow coloration. Doping with Fe and with FeGa, also removes the yellow color, but the absorption cut-off is between 3 eV and 3.3 eV. It appears that the cut-off is due to an internal transition in the Fe, perhaps from the ground, spin 5/2 state, to the spin 3/2 excited state. Thermal excitation from the excited state at room temperature could then be responsible for the “winking” phenomena observed in the Fe-doped and FeGa-doped samples.

Photorefractive measurements show interesting trends in the temperature dependence of the Fe-doped and FeGa-doped samples. The mechanisms responsible for the change in the refracted signal strength at lower temperatures in the Fe-doped sample appear to be the same as those postulated for the absorption results. The FeGa-doped sample, however, shows unexpected behavior. The results show a mixing of two “competing” acceptor states located between 3 eV and 3.3 eV.

REFERENCES

1. A.M. Glass, *Opt. Eng.* **17**, 471 (1978)
2. M.B. Klein and R.N. Schwartz, *J. Opt. Soc. Am.* **B3**, 293(1986)
3. F. Vachss and L. Hesselink, *J. Opt. Soc. Am.* **B4**, 325 (1987)
4. J.P. Huignard, J.P. Herriau, and T. Valentin, *Appl. Optics*, **16**, 2769 (1977)
5. D.M. Pepper and A. Yariv, *Optics Lett.* **5**, 59 (1980)
6. P. Gunther, *Physics Reports* **93**, 199 (1982)
7. J.F. Nye, "Physical Properties of Crystals", 242, Oxford University Press, New York(1985).
8. A. Ashkin, G.D. Boyd, J.M. Dziedzic, R.J. Smith, A.A. Ballmann, H.J. Levinstein, and K. Nassau, *Appl. Phys. Lett.* **9**, 72 (1966).
9. I. Arizmendi, J.M. Cabrera, and F. Aguillo-Lopez, *J. Optoelectronics* **7**, 149 (1992)
10. F.S. Chen, J.T. LaMacchia and D.B. Frazer, *Appl. Phys. Lett.* **13**, 223 (1968)
11. B.C. Grabmaier, R. Oberschmid, *Phys. Status Solidi (a)* **96**,199 (1986)
12. S.C. Abrahams, P.B. Jamielson, and J.L. Bernstein, *J. Chem. Phys.*, **47**, 4034 (1967)
13. M.G. Jani and L.E. Halliburton, *J. Appl. Phys.* **64**, 2022 (1988)
14. J.J. Martin, I. Foldvari, and C.A. Hunt, *J. Appl. Phys.* **70**, 7554 (1991)
15. M.T. Harris, J.J. Larkin, and J.J. Martin, *Appl. Phys. Lett.* **60**, 2162 (1992)
16. S.L. Hou, R.B. Lauer, and R.E. Aldrich, *J. Appl. Phys.* **44**, 2652 (1973)
17. R. Oberschmidt, *Phys. Status Solidi (a)* **89**, 263 (1985)
18. D.C. Craig and N.C. Stephenson, *J. Solid State Chem.* **15**, 1 (1975)
19. P.J. Picone, *J. Crystal Growth* **87**, 149 (1988)
20. D.W. Hart, C.A. Hunt, and J.J. Martin, *J. Appl. Phys.* **73**, 3974 (1993)

21. T.M. Wilson, Oklahoma State University, Stillwater, OK 74078 (private communication, June 1994)
22. I. Foldvari, J.J. Martin, C.A. Hunt, R.C. Powell, R.J. Reeves, and S.A. Holmstrom, *Optical Materials* **2**, 25 (1993)
23. G. Brost, Rome Labs, Griffiths AFB (private communication, May 1994)

APPENDIX A

DVM DATA ACQUISITION PROGRAM LISTING

```

10 CLEAR SCREEN
20 PRINT "THIS PROGRAM GRAPHS REALTIME DVM DATA"
30 DEG
40 ASSIGN @Isc TO 7
50 ASSIGN @Shutter TO 706 !PS PROG FOR SHUTTER TRIGGER
60 OPTION BASE 1
70 DIM T(1000),Sig(1000)
80 ON KEY 1 LABEL "AXES" GOSUB Grafaxes
90 ON KEY 2 LABEL "DATA" GOSUB Takedata
100 ON KEY 3 LABEL "Dump" GOSUB Dumpgraf
110 ON KEY 4 LABEL "STORE" GOSUB Storedata
120 KEY LABELS ON
130 INPUT "ENTER THE DRIVE & DIRECTORY AS:DR:\DIR\",Dr$
140 GOTO 140
150 Grafaxes: !DRAWS THE AXES ON THE SCREEN
160 !SETUP THE SHUTTER
170 CLEAR SCREEN
180 INPUT "PLEASE TELL ME THE TIME INTERVAL FOR THE SHUTTER",Tshut
190 PRINT "REMEMBER TO ENTER THE SHUTTER TIME IN THE CONTROL BOX"
200 IMAGE "THE SHUTTER TIME IS",4D.D
210 PRINT USING 200;Tshut
220 INPUT "ENTER THE TICK SPACING FOR THE TIME AXES",Ttick
230 !SET UP AND DRAW THE GRAPH FOR REALTIME PLOTTING
240 VIEWPORT 0,100*RATIO,0,100
250 WINDOW -.2*Tshut,1.05*Tshut,-15,15
260 CLIP 0,Tshut,-10,10
270 AXES Ttick,1,0,0
280 CLIP OFF
290 LORG 6
300 FOR Tm=0 TO Tshut STEP Ttick
310 MOVE Tm,-.5
320 LABEL Tm
330 NEXT Tm
340 MOVE Tshut/2,-2
350 LABEL "TIME"
360 LORG 8
370 FOR Sg=-10 TO 10 STEP 4
380 MOVE -.5,Sg
390 LABEL Sg
400 NEXT Sg
410 LDIR 90
420 MOVE -.05*Tshut,3
430 LABEL "SIGNAL"
440 LDIR 0
450 RETURN
460 Takedata: !TAKES THE DATA
470 INPUT "ENTER THE CURRENT AMP GAIN IN VOLTS/AMP",Gain
480 Gain=1.E+4/Gain !SCALE TO A MAX GAIN OF 1E4
490 !FIND Dvmavg
500 Dvmavg=0
510 FOR I=1 TO 20
520 ENTER 726;V
530 Dvmavg=V+Dvmavg
540 NEXT I
550 Avg=Dvmavg/20
560 !READ THE DVM AND PLOT THE DATA REALTIME
570 TO=TIMEDATE MOD 86400!SETS ZERO OF TIME SCALE
580 OUTPUT @Shutter USING "K";"2000"
590 WAIT .1
600 OUTPUT @Shutter USING "K";"2480"
610 MOVE 0,0
620 FOR I=1 TO 1000
630 ENTER 726;Sig(I)
640 Sig(I)=Gain*(Sig(I)-Avg)
650 T(I)=TIMEDATE MOD 86400-TO

```

```
660     DRAW T(I),(Sig(I)*100)
670     WAIT Tshut/1000
680     NEXT I
690     PRINT "I'M FINISHED, HIT ANOTHER KEY"
700     RETURN
710     PRINT "THE DATA IS IN THE COMPUTER, READY TO PRINT AND STORE"
720 Dumpgraf:
730         !
740         CONFIGURE DUMP TO "HP-PCL"
750         DUMP DEVICE IS 10,EXPANDED
760         DUMP GRAPHICS #10
770         PRINTER IS 10
780         PRINT CHR$(12)
790         PRINTER IS 1
800         PRINT "I'M FINISHED, HIT ANOTHER KEY"
810         RETURN
820 Storedata: !STORE DATA ON DISC
830         INPUT "ENTER THE FILE NAME--F$",F$
840         !STORE THE DVM DATA WITH EXTENSION.DVM
850         ASSIGN @File TO *
860         CREATE Dr$&F$&".DVM",2*N+1
870         ASSIGN @File TO Dr$&F$&".DVM";FORMAT ON
880         DIM A$(50)
890         IMAGE 15A
900         OUTPUT @File USING 880;"DVMDATA"
910         IMAGE 3D.2D,"",SD.DDE
920         FOR I=1 TO 500
930             OUTPUT @File USING 900;T(I),Sig(I)
940             NEXT I
950             ASSIGN @File TO *
960             PRINT "I'M FINISHED, HIT ANOTHER KEY"
970             RETURN
970     END
```



SUSAN PATRICIA HOEFLER

Candidate for the Degree of

Master of Science

**Thesis: PHOTOCROMIC AND PHOTOREFRACTIVE EFFECTS IN
BISMUTH SILICON OXIDE DOPED WITH IRON AND BISMUTH
SILICON OXIDE DOPED WITH IRON AND GALLIUM**

Major Field: Physics

Biographical:

Personal Data: Born in Omaha, Nebraska, on October 18, 1969.

Education: Graduated from Blair High School, Blair, Nebraska, in May, 1987. Recieved the Bachelor of Science degree in Physics from Creighton University, Omaha, Nebraska, in May, 1991. Completed the requirements for the Master of Science in Physics from Oklahoma State University in July, 1994.

Professional Experience: Research Education for Undergraduates, Oklahoma State University, June 1990 through July 1990. Teaching Assistant, Creighton University, August 1990 to May 1991. Graduate Teaching Assistant, Oklahoma State University, August 1991 to May 1992. Graduate Research Assistant, Oklahoma State University, May 1992 to present.

Professional Memberships: Optical Society of America, Sigma Pi Sigma, Pi Mu Epsilon.